Enhancing Structural Damage Identification Robustness to Noise and Damping With Integrated Bistable and Adaptive Piezoelectric Circuitry

Jinki Kim[1]
Department of Mechanical Engineering,
University of Michigan,
Ann Arbor, MI 48109-2125
e-mail: jinkikim@umich.edu

R. L. Harne
Department of Mechanical Engineering,
University of Michigan,
Ann Arbor, MI 48109-2125

K. W. Wang
Department of Mechanical Engineering,
University of Michigan,
Ann Arbor, MI 48109-2125

The accurate and reliable identification of damage in modern engineered structures is essential for timely corrective measures. Vibration-based damage prediction has been studied extensively by virtue of its global damage detection ability and simplicity in practical implementation. However, due to noise and damping influences, the accuracy of this method is inhibited when direct peak detection (DPD) is utilized to determine resonant frequency shifts. This research investigates an alternative method to detect frequency shifts caused by structural damage based on the utilization of strongly nonlinear bifurcation phenomena in bistable electrical circuits coupled with piezoelectric transducers integrated with the structure. It is shown that frequency shift predictions by the proposed approach are significantly less susceptible to error than DPD when realistic noise and damping levels distort the shifting resonance peaks. As implemented alongside adaptive piezoelectric circuitry with tunable inductance, the new method yields damage location and severity identification that is significantly more robust and accurate than results obtained following the DPD approach. [DOI: 10.1115/1.4028308]

Keywords: structural health monitoring, piezoelectric transducer, adaptive circuit, bistable circuit

1 Introduction and Motivation

In recent years, the imperative for monitoring health of structures has led to extensive research in damage identification approaches suitable across a wide range of civil, aerospace, and mechanical applications. A damage identification method utilizing structural dynamic responses may be generally classified by the local or global nature of the approach. Localized methods, such as those based on ultrasonic waves [1] or acoustic emission [2], have been widely studied because of their potential for high damage detection sensitivity for smaller defects. However, the transducers must often be positioned near damage sites and the sites must be accessible for verification purposes. Global methods, such as vibration-based approaches [3,4], measure damage induced changes of the time domain data or modal properties, such as natural frequencies and mode shapes. As a result, these methods have relatively large coverage area, provide a means for damage detection even when the damaged sites are inaccessible or not in the proximity of the transducer location, and are often more straightforward to implement than localized approaches. Among vibration-based methods, damage identification utilizing resonance frequency change, hereafter termed frequency shift-based methods [5,6], may be preferable to those based on mode shapes [7] or mode curvature [8], since resonance frequencies may be more easily measured even with a single sensor and are usually less contaminated by noise as compared to mode shapes [9]. Yet, frequency shift-based methods have two notable limitations: (1) a deficiency of data for accurate damage identification and (2) low sensitivity of frequency shifts due to damage effects particularly when resonances are distorted by noise and damping.

The issue of data deficiency is related to the number of practically measurable resonance frequencies which are typically far fewer than the number of degrees of freedom required for characterizing the damage via a corresponding structural model (e.g., a finite element model). As a result, the damage identification model solution is nonunique. To address this concern, approaches such as twin structure [10] and mass/stiffness addition [11] have been proposed to lend greater dynamic degrees of freedom to the structural model and reduce the underdetermined formulation of the model solution. Jiang et al. [12,13] proposed a form of mass/stiffness addition by incorporating adaptive piezoelectric circuitry into the structure to enrich the modal frequency measurements. The method introduces additional resonant frequencies and vibration modes to the integrated system and, in contrast to the prior techniques, is easier to implement due to straightforward integration of piezoelectric transducers and circuitry with the structural system. By favorably tuning the inductance values in the circuitry, a larger number of frequency responses with increased number of resonance frequency shifts are obtained. The study demonstrated that the enriched data set of resonance frequency shifts improved the ability to solve the inverse problem for accurate damage location and severity identification [12–14].

The second concern of frequency shift-based approaches is related to accurately determining the damage induced resonant frequency shifts [15,16]. Since noise and damping are inevitable in real applications, the distorted frequency shifts may be difficult or impossible to accurately measure by DPD. When the error is combined with the deficiency of the measurement data, damage prediction error can become adversely amplified [17]. To overcome this shortcoming, sensitivity enhancing control techniques have been investigated [18–20]. The approaches manipulate closed-loop eigenvalues and vectors by integrating active feedback control with the structure such that structural response changes due to damage are enhanced. Although the studies show

[1]Corresponding author.

Contributed by the Technical Committee on Vibration and Sound of ASME for publication in the Journal of Vibration and Acoustics. Manuscript received March 21, 2014; final manuscript received August 8, 2014; published online November 12, 2014. Assoc. Editor: Mohammed Daqaq.

promising ability to improve frequency shift-based methods, the sensitivity enhancing control concepts typically require multiple transducers for implementation in addition to being more cumbersome due to the active implementation.

While the adaptive piezoelectric circuitry concept is a viable resolution for the data deficiency concern of frequency shift-based damage identification approaches, the concern of frequency shift determination does not yet have an obvious remedy which is straightforward and passive to implement, and which maintains robustness due to noise and damping in the measured responses. Therefore, this research aims to develop an easily implemented frequency shift determination technique which does not require active control and is far less susceptible to noise and damping influences. In conjunction with the prior adaptive piezoelectric circuitry [12–14], this study investigates a new means for structural damage identification which is found to be notably robust when response signals are distorted due to realistic noise and damping, factors which otherwise degrade the viability of frequency shift determination by traditional peak detection. Although correct frequency shift determination is a principal aim of the proposed alternative approach, this study provides additional focus on the final damage identification as an unambiguous metric of success because reducing error in frequency shift prediction may not correlate to an equally improving identification of damage location and severity.

Sections 2 and 3 overview the damage identification method utilized in this study and introduce the new approach adopted for frequency shift detection. Then, a series of damage identification case studies are conducted, using a modeled structure having mild or greater damping, where both scenarios are moreover considered with and without additive noise. Following the investigations, concluding remarks reflect upon the potential of the new approach and its successful integration into the complete damage identification routine.

2 Overview of Damage Identification Using Integrated Adaptive Piezoelectric Circuitry

This section reviews the prior development of identifying damage location and severity by the frequency shift-based method using integrated adaptive piezoelectric circuitry for data enrichment, stemming from the work of Jiang et al. [12,13]. Readers interested in further model development details should refer to Refs. [12] and [13]. Figure 1 shows a schematic of the integrated electromechanical system. Based on a finite element model, the equations of motion can be written as [21]

$$\begin{bmatrix} \boldsymbol{M}_s & \boldsymbol{0} \\ \boldsymbol{0} & \boldsymbol{L} \end{bmatrix} \begin{Bmatrix} \ddot{\boldsymbol{q}} \\ \ddot{\boldsymbol{Q}} \end{Bmatrix} + \begin{bmatrix} \boldsymbol{C} & \boldsymbol{0} \\ \boldsymbol{0} & \boldsymbol{R} \end{bmatrix} \begin{Bmatrix} \dot{\boldsymbol{q}} \\ \dot{\boldsymbol{Q}} \end{Bmatrix} + \begin{bmatrix} \boldsymbol{K}_s & \boldsymbol{K}_c \\ \boldsymbol{K}_c^T & \boldsymbol{K}_p \end{bmatrix} \begin{Bmatrix} \boldsymbol{q} \\ \boldsymbol{Q} \end{Bmatrix} = \begin{Bmatrix} \boldsymbol{0} \\ \boldsymbol{V}_e \end{Bmatrix} \quad (1)$$

where $\boldsymbol{q}$, $\boldsymbol{M}_s$, $\boldsymbol{C}$, and $\boldsymbol{K}_s$ are the displacement vector, mass, damping, and stiffness matrices of the mechanical structure, respectively, and $\boldsymbol{Q}$, $\boldsymbol{L}$, $\boldsymbol{R}$, and $\boldsymbol{K}_p$ are the electrical charge flow vector, inductance, resistance, and inverse capacitance matrices of the circuit, respectively. $\boldsymbol{K}_c$ is the coupling term between mechanical and electrical domains, and $\boldsymbol{V}_e$ is the excitation voltage input. From Eq. (1), the following eigenvalue problem may be obtained:

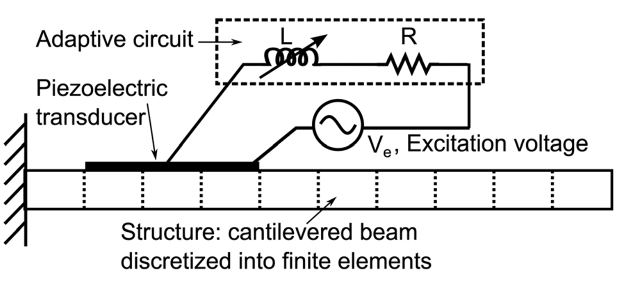

Fig. 1 Illustration of monitored structure with piezoelectric transducer and adaptive circuitry

$$\left(-\lambda_i \widetilde{\boldsymbol{M}} + \widetilde{\boldsymbol{K}}\right)\{\boldsymbol{\phi}_i\} = 0, \quad \text{where } i = 1, 2, ., N_{el} \quad (2a)$$

$$\widetilde{\boldsymbol{M}} = \begin{bmatrix} \boldsymbol{M}_s & \boldsymbol{0} \\ \boldsymbol{0} & \boldsymbol{L} \end{bmatrix}, \quad \widetilde{\boldsymbol{K}} = \begin{bmatrix} \boldsymbol{K}_s & \boldsymbol{K}_c \\ \boldsymbol{K}_c^T & \boldsymbol{K}_p \end{bmatrix} \quad (2b)$$

where λ_i and $\{\boldsymbol{\phi}_i\}$ are the ith eigenvalue and -vector, respectively, $\widetilde{\boldsymbol{M}}$ and $\widetilde{\boldsymbol{K}}$ are the generalized mass and stiffness matrices of the undamaged system with boundary conditions applied, respectively; and N_{el} is the number of discretized elements in the finite element model. By similar development, the eigenvalue problem for the damaged structure is formulated

$$\left(-\lambda_i^{dam} \widetilde{\boldsymbol{M}}^{dam} + \widetilde{\boldsymbol{K}}^{dam}\right)\left\{\boldsymbol{\phi}_i^{dam}\right\} = 0, \quad \text{where } i = 1, 2, \ldots, N_{el} \quad (3)$$

where λ_i^{dam} and $\left\{\boldsymbol{\phi}_i^{dam}\right\}$ are the ith eigenvalue and -vector of the damaged system, respectively.

By manipulating Eq. (2a), it is possible to derive the sensitivity matrix $\boldsymbol{S}$ of eigenvalue change $\{\delta\boldsymbol{\lambda}\}$ with respect to variation in elemental stiffness parameters $\{\delta\boldsymbol{d}\}$ [12]

$$-\{\delta\boldsymbol{\lambda}\} = \boldsymbol{S}\{\delta\boldsymbol{d}\} \quad (4a)$$

$$\{\delta\boldsymbol{\lambda}\} = [\delta\lambda_1, \delta\lambda_2, \ldots, \delta\lambda_m]^T \quad (4b)$$

$$\{\delta\boldsymbol{d}\} = [\delta d_1, \delta d_2, \ldots, \delta d_{N_{el}}]^T \quad (4c)$$

$$S_{ij} = \{\boldsymbol{\phi}_i\}^T \widetilde{\boldsymbol{K}}_j^T \{\boldsymbol{\phi}_i\}, \quad i = 1, 2, \ldots, m, \quad j = 1, 2, \ldots, N_{el} \quad (4d)$$

where m is the number of measured resonant frequencies of the integrated system.

Equation (4a) is usually significantly underdetermined ($m < N_{el}$), which results in erroneous damage identification. However, Jiang et al. [12,13] demonstrated that by selectively tuning the inductance, it is possible to alter the dynamics of the integrated system to obtain a suite of resonance frequency shifts due to the same structural damage. In this way, a set of altered inverse equations are obtained,

$$\begin{Bmatrix} -\delta\boldsymbol{\lambda}(L_1) \\ -\delta\boldsymbol{\lambda}(L_2) \\ \vdots \\ -\delta\boldsymbol{\lambda}(L_n) \end{Bmatrix} = \begin{bmatrix} \boldsymbol{S}(L_1) \\ \boldsymbol{S}(L_2) \\ \vdots \\ \boldsymbol{S}(L_n) \end{bmatrix} \{\delta\boldsymbol{d}\} \quad (5)$$

The merit of employing the tunable adaptive piezoelectric circuitry may be observed from Eq. (5). Since n inductance values are applied to the circuitry, the number of resonance frequency measurements can be increased to $n \times m$, and thus the inverse problem becomes much less underdetermined. Given correct frequency shift determination throughout the enriched data set, related to the eigenvalue changes $\delta\boldsymbol{\lambda}$, accurate damage identification is then more readily achieved. Additionally, due to the global nature of the vibration-based detection method, the past studies observed an insensitivity of the method's accuracy as related to the piezoelectric transducer position with respect to the damage site [12,13], which highlights the versatility of the approach.

3 Bifurcation-Based (BB) Detection of Frequency Shifts

3.1 BB Sensing. The data enrichment routine by inductance tuning with the adaptive piezoelectric circuitry, therefore, requires determination of a suite of frequency shifts. Direct peak detection (DPD) is a straightforward means to extract resonant frequency shifts due to structural changes, but the accuracy of the approach greatly degrades when noise and damping distort response signals. As will be shown, even mild damping and low-level noise can lead to significant error for damage identification if employing DPD for determination of frequency shifts.

To surmount these concerns, this research develops an alternative approach for frequency shift detection based upon bifurcation phenomena associated with strongly nonlinear dynamic systems. The term bifurcation denotes a sudden qualitative change of response in consequence to infinitesimal parameter change. In fundamental physics studies, bifurcations have been utilized in the Josephson bifurcation amplifier to detect otherwise imperceptible shifts in current level [22]. In microscale mass sensing, change in resonance frequency of MEMS is tracked by activating bifurcations of the sensors in consequence to minute adsorption of the target analyte mass [23–26].

Studies in the context of MEMS mass sensing have shown that frequency shift-tracking using bifurcations is much less susceptible to deteriorating performance due to measurement noise and damping than traditional DPD [23]. This is because change in environmental damping may be rectified in a BB sensing method by adjustment of the excitation amplitude which does not similarly alleviate accuracy concerns for DPD, particularly on the microscale [23]. The comparable objectives of this work, albeit on much larger scales, encourage the present adoption of bifurcations for structural health monitoring applications. However, a notable distinction between micro- and macro-scale structures makes direct implementation of bifurcations for structural sensing a challenge: the existence of strong nonlinearity.

Nonlinear responses for microscale sensors are common due to geometry and material effects, even before higher excitation levels drive the structures to nonlinear regimes [27]. In contrast, it is atypical for mechanical or civil structures that are monitored for damage to undergo strongly nonlinear behaviors. As a result, other means must be introduced to harness bifurcations on larger structural scales. Recently, Harne and Wang [28] explored an integration of the monitored structure with piezoelectric transducer and bistable circuitry. The composite system enabled the detection of structural change (mass addition) due to activation of circuitry bifurcations. As compared to the monitored structural system exhibiting strongly nonlinear behaviors, the bifurcations used for change detection are strictly a matter of the strongly nonlinear bistable circuitry which has negligible back-coupling to the host structure response. Observing the utility of the structure and bistable circuit integration in Ref. [28], this research adopts a similar configuration in tandem with the adaptive piezoelectric circuitry to track the structural frequency shifts induced due to damage. By utilizing the voltage measured from the piezoelectric transducer with the adaptive circuitry approach as the input voltage for the bistable circuit, the host structural spectral change induced by damage can be assessed by the activation of circuitry bifurcations. Thus, the proposed sensing framework introduces the required strong nonlinearity via the attachment or inclusion of bistable circuitry into the damage detection process. Therefore, the aims of this study are to investigate the viability of the system integration and its robustness and accuracy in the presence of realistic noise and damping as compared to traditional peak detection approaches.

3.2 Overview of BB Frequency Shift Detection Procedure.

This section describes a procedure to monitor frequency shifts when utilizing bistable circuitry bifurcations. Figure 2 shows the bistable circuit employed in this study and the essential components of the structural integration: excited host structure to be monitored, piezoelectric transducer, and electrical connection from the transducer to serve as input voltage V_b for the bistable circuit having output voltage V_o. For low input voltage level, the bistable circuit undergoes small amplitude, intrawell oscillations of output level; whereas higher input levels may trigger energetic, interwell oscillations. Figure 3(a) plots an experimental contour

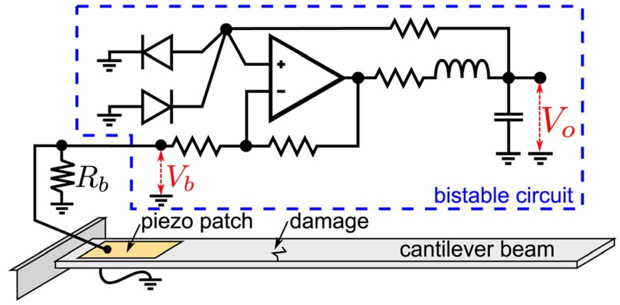

Fig. 2 Schematic of excited host structure to be monitored with piezoelectric transducer and attached bistable circuitry, as adapted and replotted from the authors' previous study [28]

of bistable circuit output-to-input voltage frequency response function (frf) magnitude as function of excitation frequency and level, as adapted and replotted from the authors' previous study [28]. For constant excitation frequency, an increasing input voltage level may activate the bifurcation leading to dramatic change in output response level, from intra- to inter-well response, or vice versa. The quantitative and qualitative differences between typical measured intra- to interwell circuit output voltage responses are shown in Figs. 3(b) and 3(c). An approximate demarcation boundary between the two steady-state response regimes is denoted in Fig. 3(a) by the light dashed curve. By tuning bistable circuit component values, the frequency sensitivity of the sudden change in circuit output voltage amplitude can be designed to target a specific structural mode. In Fig. 3(a), the sensitive region is located around excitation frequencies 7–10 Hz, where small changes in input voltage level around 0.34 V activate a saddle-node bifurcation in output voltage level. This region of sensitive bistable circuit response is that exploited in the present research.

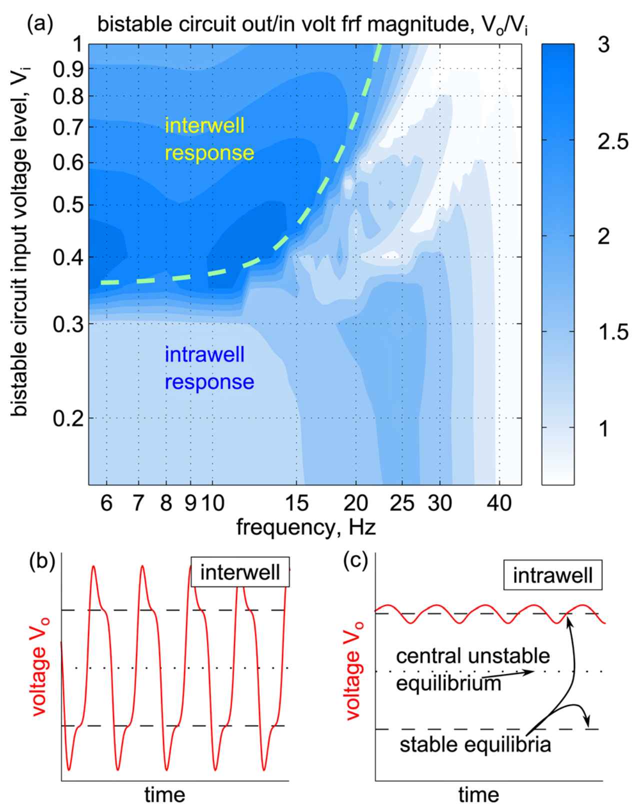

Fig. 3 (*a*) Experimental bistable circuit response, as function of excitation frequency and level, as adapted and replotted from the authors' previous study [28]. Example experimental voltage time series for (*b*) interwell and (*c*) intrawell dynamics.

Through the strategic integration of the structure and bistable circuitry, the structural responses effectively become the input voltage level to the circuit, which is exploited to detect and measure frequency shifts in resonance peaks using the overall procedure illustrated in Fig. 4. The host structural responses before and after damage, measured via the piezoelectric transducer, are used as discrete input voltage levels to the bistable circuit following adjustment of gain and frequency sensitivity. The tuning resistance R_b linearly adjusts the amplitude of the structural response measurements from the piezoelectric transducer such that an activation threshold is aligned with an intermediate amplitude of the resonance, and sets this level to be the critical level that may activate the bistable circuit bifurcations. In Fig. 3, this critical level is seen to be approximately 0.34 V, and in Fig. 4(*a*) the resonance peak amplitude has been adjusted by tuning the gain such that a portion of the peak is above this critical input voltage level. The frequency sensitivity is adjusted such that the favorable threshold bandwidth is shifted to occur around the structural mode being monitored (i.e., shifting the comparable bandwidth of 7–10 Hz in Fig. 3 to the bandwidth around the resonance of interest).

The method to determine frequency shifts with the bistable circuitry may be conducted online or offline. So long as the strategies may be carried out with equal success in meeting the implementation assumptions, the online and offline frequency shift determination strategies should be equally valid due to the findings of the past research [28] which indicated the bistable circuit design leads to negligible back-coupling to the host structure response. When employing the offline implementation, the spectral amplitudes of host structural response (whether excited naturally or by direct methods) are computed from measurements taken without connection to the bistable circuit. Then, the corresponding voltage level for each frequency after the gain adjustment is utilized as input signal to the bistable circuit. In the online execution of the approach, the structure is excited at a single frequency and the response from the piezoelectric transducer is directly fed to the bistable circuit following gain adjustment; such direct integration of the electrical and mechanical domains is that depicted in Fig. 2. The steady-state circuit output voltage response is then evaluated for whether it obtained intra- or inter-well oscillations, as illustrated by comparable intra- and inter-well responses of the bistable circuit shown in Figs. 3(*b*) and 3(*c*). Repeating this process across the spectrum containing the resonance frequency yields two bifurcations in response: one up and one down in circuit output voltage level. Repeating this process again for the damaged structural responses yields two more bifurcations at certain frequencies. Figure 4(*b*) presents example output results from this overall procedure indicating that over certain bandwidths the interwell responses are activated whereas across other frequencies the intrawell responses were obtained. Thus, from healthy to damaged states, two shifts in frequency are acquired, shown in Fig. 4(*b*): one corresponding to the jumps up in output voltage level and one corresponding to the drops down in level. In this investigation, all of the following results utilize the mean of the two frequency shifts which is considered to be the damage induced frequency shift of the resonance. Moreover, repeating this process using different gain adjustment or bistable circuit parameters (e.g., resistance or inductance) leads to still further frequency shifts, all of which may be taken into consideration when determining a mean frequency shift from healthy to damage structural states which can increase the confidence that the final result is the true frequency shift. By these procedures, the multiple frequency shifts induced by damage may be quantified and employed in the damage identification routine.

4 Verification of BB Detection of Frequency Shifts

In this section, the viability of the BB approach is assessed as compared to DPD. Because the earlier research [28] observed good agreement between the numerically predicted and experimentally measured responses of the bistable circuit and the host structure, this research conducts the following damage identification studies using the same bistable circuit model formulation. The configuration considered of a cantilever beam with integrated bistable and adaptive piezoelectric circuit network is shown in Fig. 5(*a*), which specifically represents the online implementation of the frequency shift determination strategy based upon the BB method. The beam is evenly discretized into ten finite elements and the piezoelectric transducer is considered to be perfectly bonded to the top surface of the beam from the second to fourth element. The transducer is connected to a tunable inductive circuit with a resistor R. Without loss of generality, damage is represented by 15% structural stiffness reduction on the second element in the finite element model of the beam; note that this element position concurrently indicates the modeled physical position of

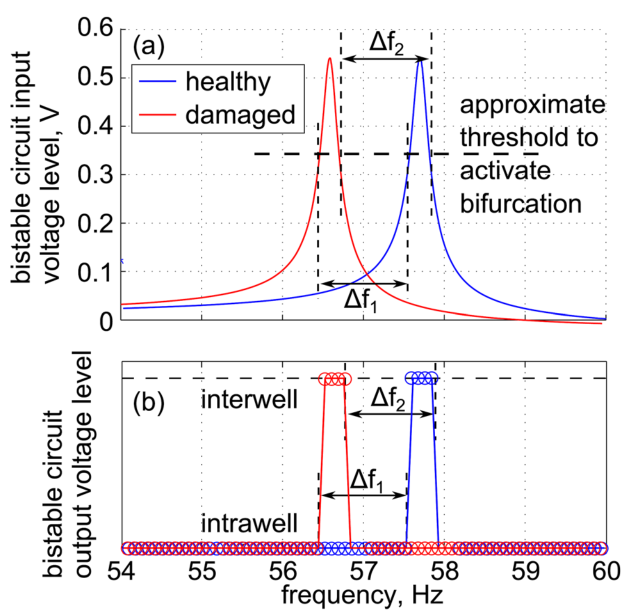

Fig. 4 (*a*) Bistable circuit input voltage level. (*b*) Representative output voltage level triggering profile across the spectrum for healthy and damaged structures.

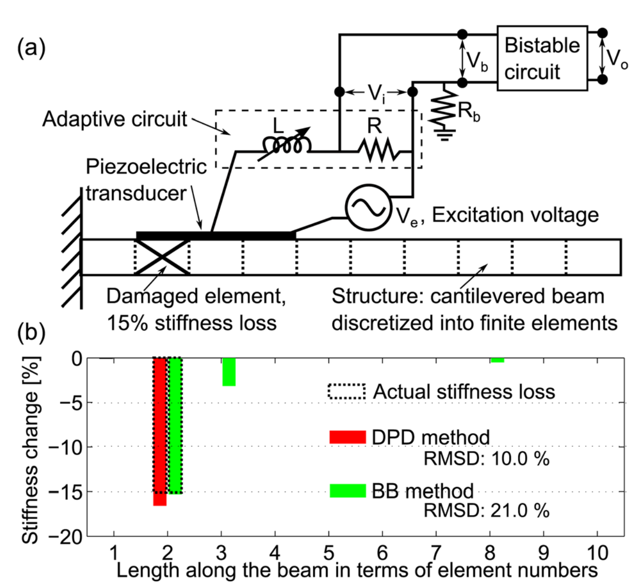

Fig. 5 (*a*) Configuration of the cantilever beam integrated with bistable and adaptive piezoelectric circuitry. (*b*) Identification of damage on second element of the beam.

Table 1 System parameters

Beam structure		Piezoelectric material	
Length	209.2 mm	Length	62.8 mm
Thickness	3.175 mm	Thickness	0.191 mm
Width	38.1 mm	Young's modulus	66 GPa
Young's modulus	71 GPa	Density	7800 kg/m^3
Loss factor	0.3%	Dielectric constant, β_{33}	7.1445 $\times 10^{-7}$ V·m/C
Density	2700 kg/m^3	Piezoelectric constant, h_{31}	1.0707 $\times 10^{9}$ N/C

the structural damage. Relevant parameters used in the damage identification model are listed in Table 1.

The proposed damage identification approach is summarized as follows. The healthy structure is first evaluated as a baseline. The excitation voltage V_e is swept over the chosen frequency range, and the response levels of the electromechanical system are measured as voltage drops V_i across resistor R. Around each natural frequency of interest, the amplitudes of voltage V_i are scaled to a suitable level by tuning resistor R_b, and this signal is the excitation for the bistable circuit V_b. The activation of bistable circuit bifurcations is then evaluated by analyzing the output voltage level V_o of the bistable circuit as described in Sec. 3.2. Then, the inductance of the adaptive circuit is selectively tuned following the procedure of Jiang et al. [12,13], and the process is repeated for a desired number of inductances to enrich the data set. Once completed, this forms the data set of bifurcation frequencies for the healthy, baseline structure. Following damage, the process is repeated, yielding a second data set of bifurcation frequencies. The difference between the data sets of bifurcation frequencies is therefore the collection of frequency shifts to be used in the damage identification routine described in Sec. 2. To comment on practical implementation of the online and offline implementations of the BB method, for an ideal op-amp junction in the bistable circuit shown in Fig. 2 no backward coupling of electrical response will occur to influence the voltage V_i across resistor R [28]. In practice, very small coupling will exist for an online implementation of the BB method. To fully eliminate this concern and to ensure that undesired measured structural responses do not impede the reliability of activating the bistable circuit bifurcations, offline BB frequency shift detection can be implemented as detailed in Sec. 3.2.

In this initial evaluation, the response signals are free of additive noise. The data set of first three resonance frequency shifts is enriched by selecting 14 tunable inductances, yielding a total of 42 shifts. The resonance frequency shifts are determined by conventional DPD and the proposed BB approach. In the following studies, the BB method was implemented with numerical simulations of the bistable circuit responses using the governing equations formulated in Ref. [28] and random initial conditions. The DPD results were likewise generated by direct computation. Then, damage is identified and prediction results are compared.

The resonance frequency shifts as determined by BB and DPD approaches are given in Table 2. The frequency shifts obtained by DPD are considered to be accurate because no noise is included in the investigation. Due to the selection of inductances, the first and second resonance frequencies of the integrated system vary significantly when the inductance is tuned around 40.0 H; the second and third resonances change when the inductance is tuned around 1.04 H. The multiple frequency shifts acquired by either DPD or BB approaches indicate that information about damage is enriched which reduces the underdetermined formulation of Eq. (5) for damage identification. Table 2 shows that the frequency shifts detected by BB and DPD methods exhibit little absolute difference. The mean and standard deviation of the differences are −0.01 and 0.05 Hz, respectively, while the maximum difference is 0.15 Hz.

Figure 5(*b*) presents the damage location and severity predictions following BB or DPD frequency shift detection. It is seen that the results from DPD and BB methods both predict close to the actual 15% stiffness loss at the second element. Root-mean-square deviation (RMSD) between the predicted stiffness reduction $\delta \boldsymbol{d}^{\text{predict}}$ and the actual damage $\delta \boldsymbol{d}^{\text{actual}}$ is employed as a metric to quantify prediction error

$$\text{RMSD} = \sqrt{\frac{\sum_{i=1}^{N_{\text{el}}} \left(\delta d_i^{\text{predict}} - \delta d_i^{\text{actual}}\right)^2}{\sum_{i=1}^{N_{\text{el}}} \left(\delta d_i^{\text{actual}}\right)^2}} \tag{6}$$

RMSD by DPD and BB method both showed relatively small error levels: 10.0% and 21.0%, respectively. From these results, it can be concluded that the BB method shows comparable performance to the traditional DPD strategy with respect to frequency shift determination and final damage identification when the response signals are free of noise.

Table 2 Damage induced resonance frequency shifts measured by DPD and BB methods under inductance tuning

	First resonance frequency shift (Hz)			Second resonance frequency shift (Hz)			Third resonance frequency shift (Hz)		
Inductance (H)	DPD	BB	Difference	DPD	BB	Difference	DPD	BB	Difference
0.89	1.32	1.34	−0.02	1.22	1.37	−0.15	0.14	0.10	0.04
0.94	1.32	1.33	−0.01	1.16	1.25	−0.09	0.19	0.25	−0.06
0.99	1.32	1.31	0.01	1.01	1.13	−0.12	0.38	0.52	−0.13
1.04	1.32	1.31	0.01	0.44	0.52	−0.08	0.97	1.02	−0.05
1.09	1.33	1.32	0.01	0.05	0.13	−0.08	1.28	1.31	−0.03
1.14	1.30	1.29	0.01	0.03	0.06	−0.03	1.33	1.33	0.00
1.19	1.31	1.31	0.00	0.02	0.06	−0.04	1.33	1.32	0.01
32.5	1.20	1.20	0.00	0.12	0.09	0.03	1.31	1.18	0.13
35.0	1.10	1.10	0.00	0.19	0.21	−0.02	1.31	1.31	0.00
37.5	1.00	1.00	0.00	0.29	0.30	−0.01	1.32	1.31	0.01
40.0	0.87	0.87	0.00	0.45	0.43	0.02	1.31	1.30	0.01
42.5	0.73	0.73	0.00	0.58	0.61	−0.03	1.31	1.28	0.03
45.0	0.59	0.60	−0.01	0.72	0.71	0.01	1.31	1.22	0.09
47.5	0.48	0.48	0.00	0.82	0.82	0.00	1.31	1.23	0.08

5 Improving Accuracy of BB Frequency Shift Detection Through Greater Number of Evaluations

Section 4 employed a single run of the BB frequency shift detection procedure for use in the damage identification routine. It was found that the identification results following noise-free BB frequency shift determination slightly differed from the DPD approach. Because dynamics associated with the saddle-node bifurcation used in this research are sensitive to initial conditions, and thus activation of the bifurcations may be slightly inconsistent from one time series circuit simulation to the next, it may be anticipated that increased number of runs using randomly selected initial conditions to determine a greater number of frequency shifts may improve confidence in the BB damage identification result. With greater number of runs, the final mean value of detected frequency shift may then be used in the damage identification routine.

Therefore, using the model of Sec. 4, the BB frequency shift detection procedure was carried out for 40 runs with random initial conditions covering several multiples of the stable equilibria of output voltage level (± 1 V) to ensure sufficient sampling of the initial condition parameter space. The mean and first standard deviation of the resulting frequency shifts determined by the BB method are plotted in Fig. 6(*a*) (circles and error bars) as compared to the actual resonance frequency shifts (squares), considered to be the DPD method values. The horizontal axis indicates the inductance values used for the data enrichment routine. The individual shifts determined from all 40 runs for each inductance are plotted as crosses. For conciseness, results from the first resonance peak are plotted; results from the remaining two resonances are comparable. As shown in Fig. 6(*a*), the actual resonance frequency shifts are within 1 standard deviation of the BB method mean shift, and the BB method accurately tracks the shifts as inductance is tuned to enrich the data set for the damage identification routine.

The means of the 40 frequency shifts for each of the three shifting resonance frequencies were then utilized for damage identification; the results are provided in Fig. 6(*b*). The accuracy of damage predicted by the mean of 40 runs is improved from that computed from a single run: the RMSD is reduced from 21.0% to 14.4%. The results indicate that greater number of runs using the BB method may enhance the accuracy of frequency shift determination. Practically, conducting increased number of runs using the online implementation approach of the BB method may be a time-consuming procedure. However, the additional time necessary for increased number of runs is less of a concern in the offline approach since the method may be conducted numerically, as done in this research, and take advantage of parallel computing architectures to greatly expedite the process.

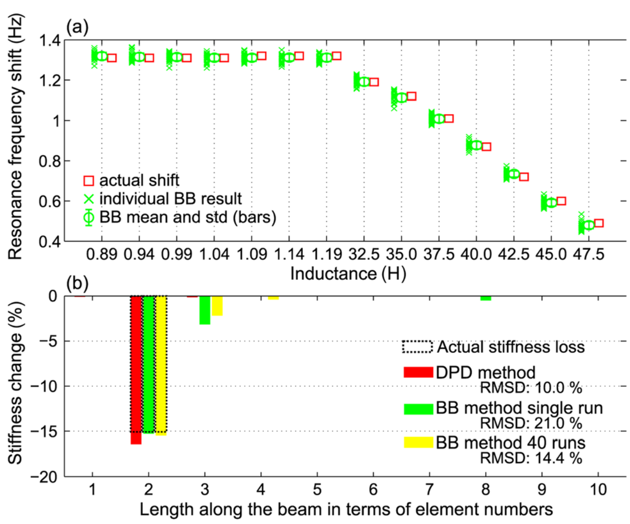

Fig. 6 (*a*) Frequency shifts determined by 40 runs of BB method each having random initial conditions for each inductance. (*b*) Damage identification using the mean results from the 40 resonance frequency shifts.

6 Investigation of Noise Influences

6.1 Case Study 1: Structure With Mild Damping. Sections 4 and 5 evaluated BB frequency shift determination when the response signals from the structure and adaptive piezoelectric circuitry network were free of noise. However, measurement noise is oftentimes unavoidable due to factors including piezoelectric transducer bonding, fidelity of wires and electrical components, electromagnetic radiation, and ground loops. Therefore, this section investigates the addition of low-pass filtered noise, ranging from 44 to 32 dB signal-to-noise ratio (SNR), with the response signals of Secs. 4 and 5 to assess how detection of frequency shifts by DPD and BB methods are affected and how the final damage identification results are influenced. To appreciate the low-level of noises employed, Fig. 7 plots a comparison of an example response resonance used in the following investigation for the noise-free case and that with 32 dB SNR additive low-pass filtered noise which is the highest level utilized in these case studies. In practice, such low-level noise could be caused by conventional sensor sensitivity constraints [29,30].

The investigation of Sec. 4 was then repeated but now, with each case of inductance tuning, low-pass filtered white noise is added to the response signals. Thus, for each of the 14 inductance tuning cases, different frequency shifts for the three resonance peaks may be determined following both DPD and BB methods should noise influence the results. For each scenario, a single run of the BB frequency shift detection method is employed and, likewise, the DPD approach is utilized with a structural response spectra distorted by the same randomly generated additive noise. Figure 8 plots the frequency shift error showing the 42 individual results (crosses) for each case of noise and detection method, while the mean values are shown as circles with first standard deviations indicated by error bars. The numerical values of first standard deviation are given alongside each case.

As detailed in Secs. 4 and 5, the frequency shifts determined by the BB approach when the responses are noise-free exhibit a small but finite spread of values and thus a small range of errors. However, as noise is added to the response signals, the deviations of the frequency shifts by the BB method remain small and steady while those determined by DPD grow significantly, even for the lowest level of noise. Figure 9 presents the corresponding damage identification results. Figure 9(*a*) shows that damage location results by DPD alter dramatically with the addition of the lowest level of noise; although the DPD method still correctly predicts approximately 15% stiffness reduction at the second element, now

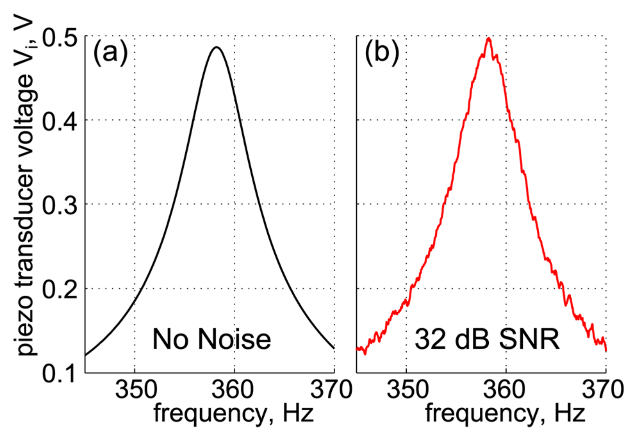

Fig. 7 Example of (*a*) noise-free integrated system resonance and (*b*) that with 32 dB SNR additive noise

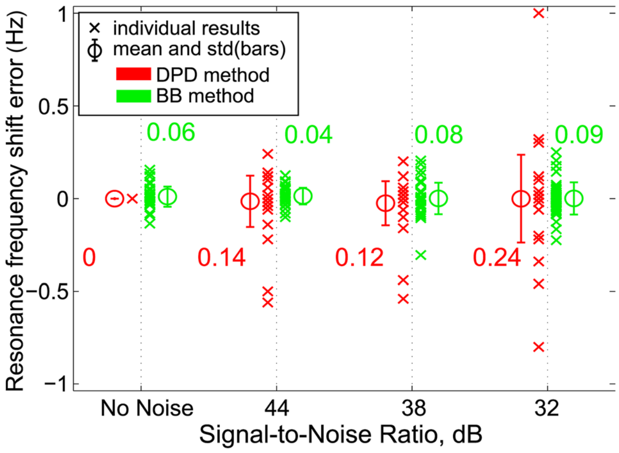

Fig. 8 Frequency shifts determined by DPD or BB approaches and their standard deviations as SNR increases

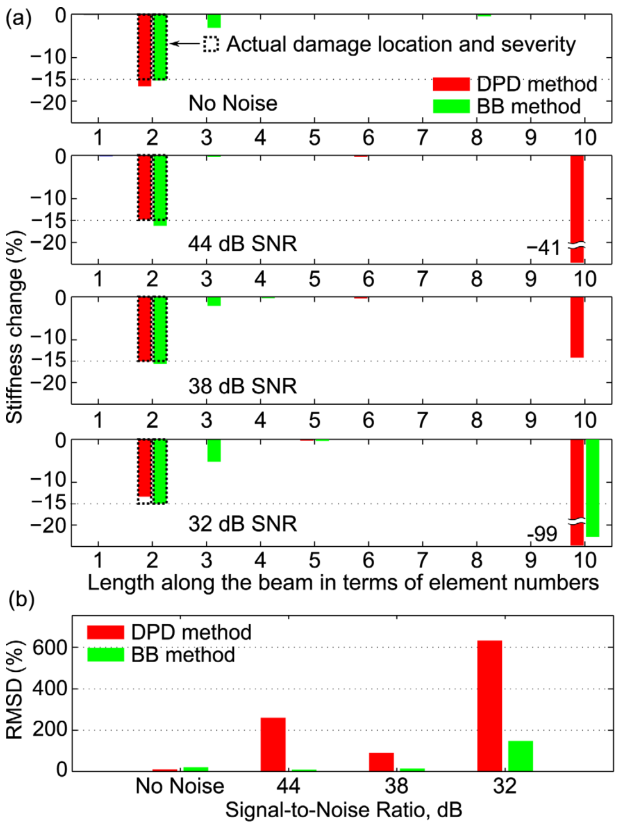

Fig. 9 (*a*) Damage identification comparison for structure with mild damping and with varying degrees of low-level additive noise. (*b*) RMSD of damage identification.

a 41% stiffness reduction is estimated at the tenth element. Since structural health monitoring systems may not distinguish false from accurate damage identification, the incorrect DPD predictions may mislead corrective measures. Figure 9(*b*) presents the RMSD which indicates the BB method is substantially less influenced by the noise addition and its damage identification maintains higher degree of confidence for correctness.

6.2 Case Study 2: Structure With Increased Damping. The prior investigation considered a lightly damped structure with loss factor 0.3%. While some structural systems may have such low damping in an ideal configuration, the introduction of boundary conditions, imperfections in mounting, and even structural-acoustic factors often contribute to increase damping levels in civil and mechanical structures. Thus, this section repeats the noise study of Sec. 6.1 but increases the structural loss factor from 0.3% to 0.5%.

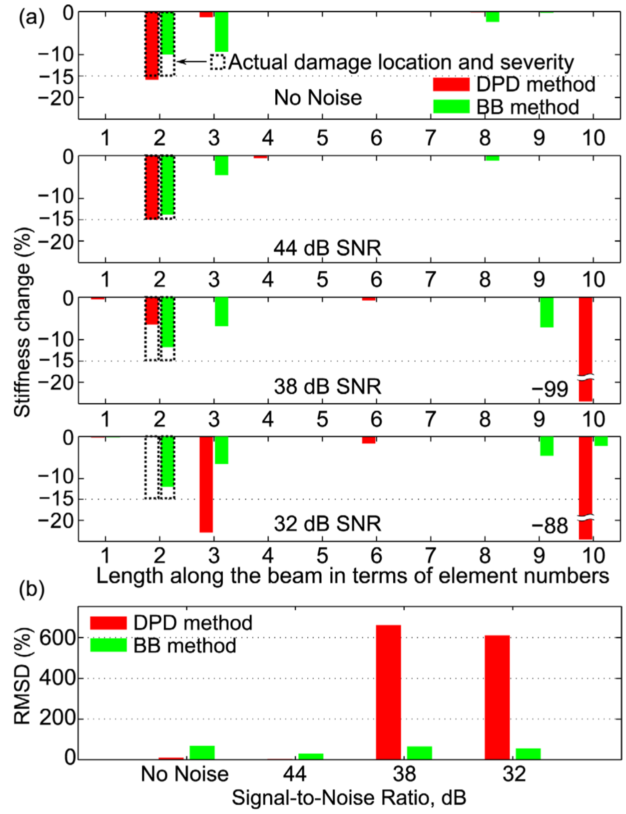

Fig. 10 (*a*) Damage identification comparison for structure with increased damping and for varying degrees of low-level additive noise. (*b*) RMSD of damage identification.

Figure 10(*a*) presents the resulting damage identification comparing DPD and BB frequency shift detection approaches as noise increases while Fig. 10(*b*) provides the corresponding RMSD. In tandem with increased structural damping levels, Fig. 10 shows that DPD-based damage identification becomes unreliable and justifies common suspicions that the approach has clear disadvantages despite its appealing ease of implementation. In contrast, the BB method for frequency shift determination provides improved robustness to noise and damping and the more accurate damage predictions attest to its advantages. While the BB method ultimately yields some predictive error, as described in Secs. 4 and 5, increasing the number of runs, using greater number of gain adjustments, or tailoring bistable circuit parameters could provide means to heighten confidence in its predictive capability and further enhance its performance for accurate damage identification.

7 Conclusions

This research investigated an integration of bistable and adaptive piezoelectric circuitry to enhance the robustness and accuracy of structural damage identification which are otherwise compromised due to noise and damping. Detecting frequency shifts via a BB strategy provides an alternative to traditional DPD. The BB method is found to be significantly less affected by the addition of noise and increased damping in the response signals and therefore provides higher level of confidence in its final damage identification results. With the BB method, increasing the number of runs, using greater number of gain adjustments, or modifying bistable circuit parameters could provide ways to determine a mean frequency shift value that may further enhance the accuracy of the damage identification. In summary, the results of this study provide new pathway for easily implemented and accurate vibration-based global damage identification.

Acknowledgment

This research was supported by the Air Force Office of Scientific Research (FA9550-11-1-0072).

References

[1] Raghavan, A., and Cesnik, C. E. S., 2007, "Review of Guided-Wave Structural Health Monitoring," Shock Vib. Dig., **39**(2), pp. 91–116.

[2] Huguet, S., Godin, N., Gaertner, R., Salmon, L., and Villard, D., 2002, "Use of Acoustic Emission to Identify Damage Modes in Glass Fibre Reinforced Polyester," Compos. Sci. Technol., **62**(10–11), pp. 1433–1444.

[3] Carden, E. P., and Fanning, P., 2004, "Vibration Based Condition Monitoring: A Review," Struct. Health Monit., **3**(4), pp. 355–377.

[4] Figueiredo, E., Park, G., Farinholt, K. M., Farrar, C. R., and Lee, J. R., 2012, "Use of Time-Series Predictive Models for Piezoelectric Active-Sensing in Structural Health Monitoring Applications," ASME J. Vib. Acoust., **134**(4), p. 041014.

[5] Salawu, O. S., 1997, "Detection of Structural Damage Through Changes in Frequency: A Review. Engineering Structures," Eng. Struct., **19**(9), pp. 718–723.

[6] Majumdar, A., Maiti, D. K., and Maity, D., 2012, "Damage Assessment of Truss Structures From Changes in Natural Frequencies Using Ant Colony Optimization," Appl. Math. Comput., **218**(19), pp. 9759–9772.

[7] Qiao, P., and Cao, M., 2008, "Waveform Fractal Dimension for Mode Shape-Based Damage Identification of Beam-Type Structures," Int. J. Solids Struct., **45**(22), pp. 5946–5961.

[8] Lestari, W., Qiao, P., and Hanagud, S., 2007, "Curvature Mode Shape-Based Damage Assessment of Carbon/Epoxy Composite Beams," J. Intell. Mater. Syst. Struct., **18**(3), pp. 189–208.

[9] Friswell, M. I., and Penny, J. E. T., 1997, "Is Damage Location Using Vibration Measurements Practical?," EUROMECH 365 International Workshop: DAMAS 97, Sheffield, UK, July 30–Aug. 2, pp. 351–362.

[10] Trivailo, P., Plotnikova, L. A., and Wood, L. A., 1997, "Enhanced Parameter Identification for Damage Detection and Structural Integrity Assessment Using Twin Structures," 5th International Congress on Sound and Vibration (ICSV5), Adelaide, Australia, Dec. 15–18, Paper No. 270, Vol. IV, pp. 1733–1741.

[11] Cha, P. D., and Gu, W., 2000, "Model Updating Using an Incomplete Set of Experimental Modes," J. Sound Vib., **233**(4), pp. 583–596.

[12] Jiang, L. J., Tang, J., and Wang, K. W., 2006, "An Enhanced Frequency-Shift-Based Damage Identification Method Using Tunable Piezoelectric Transducer Circuitry," Smart Mater. Struct., **15**(3), pp. 799–808.

[13] Jiang, L. J., Tang, J., and Wang, K. W., 2008, "On the Tuning of Variable Piezoelectric Transducer Circuitry Network for Structural Damage Identification," J. Sound Vib., **309**(3), pp. 695–717.

[14] Wang, K. W., and Tang, J., 2008, *Adaptive Structural Systems With Piezoelectric Transducer Circuitry*, Springer, New York.

[15] Farrar, C. R., Baker, W. E., Bell, T. M., Cone, K. M., Darling, T. W., Duffey, T. A., and Migliori, A., 1994, "Dynamic Characterization and Damage Detection in the I-40 Bridge Over the Rio Grande," Los Alamos National Lab, Los Alamos, NM, Technical Report No. LA-12767-MS.

[16] Chen, H. L., Spyrakos, C. C., and Venkatesh, G., 1995, "Evaluating Structural Deterioration by Dynamic Response," J. Struct. Eng., **121**(8), pp. 1197–1204.

[17] Koh, B. H., and Dyke, S. J., 2007, "Structural Health Monitoring for Flexible Bridge Structures Using Correlation and Sensitivity of Modal Data," Comput. Struct., **85**(3), pp. 117–130.

[18] Jiang, L. J., Tang, J., and Wang, K. W., 2007, "An Optimal Sensitivity-Enhancing Feedback Control Approach Via Eigenstructure Assignment for Structural Damage Identification," ASME J. Vib. Acoust., **129**(6), pp. 771–783.

[19] Jiang, L. J., and Wang, K. W., 2009, "An Experiment-Based Frequency Sensitivity Enhancing Control Approach for Structural Damage Detection," Smart Mater. Struct., **18**(6), p. 065005.

[20] Koh, B. H., and Ray, L. R., 2004, "Feedback Controller Design for Sensitivity-Based Damage Localization," J. Sound Vib., **273**(1), pp. 317–335.

[21] Tang, J., and Wang, K. W., 2004, "Vibration Confinement Via Optimal Eigenvector Assignment and Piezoelectric Networks," ASME J. Vib. Acoust., **126**(1), pp. 27–36.

[22] Vijay, R., Devoret, M. H., and Siddiqi, I., 2009, "Invited Review Article: The Josephson Bifurcation Amplifier," Rev. Sci. Instrum., **80**(11), p. 111101.

[23] Zhang, W., and Turner, K. L., 2005, "Application of Parametric Resonance Amplification in a Single-Crystal Silicon Micro-Oscillator Based Mass Sensor," Sens. Actuators A, **122**(1), pp. 23–30.

[24] Younis, M. I., and Alsaleem, F., 2009, "Exploration of New Concepts for Mass Detection in Electrostatically-Actuated Structures Based on Nonlinear Phenomena," ASME J. Comput. Nonlinear Dyn., **4**(2), p. 021010.

[25] Kumar, V., Boley, J. W., Yang, Y., Ekowaluyo, H., Miller, J. K., Chiu, G. T. C., and Rhoads, J. F., 2011, "Bifurcation-Based Mass Sensing Using Piezoelectrically-Actuated Microcantilevers," Appl. Phys. Lett., **98**(15), p. 153510.

[26] Harne, R. L., and Wang, K. W., 2014, "A Bifurcation-Based Coupled Linear-Bistable System for Microscale Mass Sensing," J. Sound Vib., **333**(8), pp. 2241–2252.

[27] Lifshitz, R., and Cross, M. C., 2008, "Nonlinear Dynamics of Nanomechanical and Micromechanical Resonators," *Reviews of Nonlinear Dynamics and Complexity*, H. G. Schuster, ed., Wiley-VCH, Weinheim, Germany, pp. 1–52.

[28] Harne, R. L., and Wang, K. W., 2013, "Robust Sensing Methodology for Detecting Change With Bistable Circuitry Dynamics Tailoring," Appl. Phys. Lett., **102**(20), p. 203506.

[29] Paek, J., Chintalapudi, K., Govindan, R., Caffrey, J., and Masri, S., 2005, "A Wireless Sensor Network for Structural Health Monitoring: Performance and Experience," Second IEEE Workshop on Embedded Networked Sensors (EmNetS-II), Washington, DC, May 30–31.

[30] Lynch, J. P., and Loh, K., 2006, "A Summary Review of Wireless Sensors and Sensor Networks for Structural Health Monitoring," Shock Vib. Dig., **38**(2), pp. 91–130.